COMPARING THE BULK COMPOSITIONS OF LUNAR GRANITES, WITH PETROLOGIC IMPLICATIONS. S. M. Seddio, R. L. Korotev, B. L. Jolliff, and R. A. Zeigler, Department of Earth and Planetary Sciences and McDonnell Center for the Space Sciences, Washington University, St. Louis, Missouri 63130 (sseddio@levee.wustl.edu).

Introduction: Because most lunar granites are not pristine, i.e., they are contaminated with non-granitic materials, mixed via impact, it is difficult to ascertain their true bulk compositions. The recent characterization of a pristine lunar granite, 12032,366-19 [1], provides an opportunity to compare it with other pristine lunar granites (Table 1). The origin of lunar granite is not well understood, and the scale on which it forms in lunar igneous environments is not known. Because 12032,366-19 is composed of a mineral assemblage consistent with late-stage fractional crystallization, it a good candidate for crystallization modeling to attempt to determine a "parent" melt, e.g., KREEP basalt or some other compositionally evolved melt. It may help elucidate whether extended fractional crystallization is sufficient to generate these granitic melts or if special circumstances such as silicate liquid immiscibility are required to explain the bulk composition.

Methods: The bulk composition of 12032,366-19 (Table 1) was determined by INAA (instrumental neutron activation analysis) in a study of 2–4-mm lithic fragments from the Apollo 12 regolith [1-4]. Phase compositions were determined by WDS electron probe microanalyses using the JEOL 8200 electron microprobe at Washington University. A modal recombination (Table 1) was performed to estimate the concentration of elements and oxides for which data were not obtained via INAA. The model was constrained to closely fit the elements and oxides for which both microprobe and INAA concentrations were obtained (FeO, CaO, BaO, Na_2O, K_2O, ZrO_2). Fractional crystallization modeling was done using the MAGFOX program of Longhi [5].

Mineralogy of 12032,36-19: The mineralogy of 12032,366-19 is unique among lunar granites. The assemblage includes graphic intergrowths of K-feldspar ($An_{1.2-6.1}$,Ab_{25-33},Or_{58-74},$Cn_{0.4-3.9}$) and quartz (determined by Raman spectroscopy), and of plagioclase (An_{35-48}, Ab_{52-64},$Or_{0.9-1.3}$,$Cn_{0.0-0.1}$) and quartz. The mafic phases are ferropyroxene ($En_{4.6-6.2}$,Fs_{51-52},Wo_{43-44}, 6.0 wt%) and fayalite ($Fo_{2.7}$,Fa_{97}, 3.1 wt% of 12032,366-19) [1]. Accessory minerals include ilmenite, ZrO_2, and two Zr-Ti-Fe-rich phases.

12032,366 and Other Pristine Lunar Granites: Compositionally, granite 12032,366-19 is most similar to samples "12013 light," [6,7,8,9], 12070,102-5 [10], 14321,1027 [11], 15405,12 [12], and 73255,27/,3 [13]. 15405,12 differs the most; it contains ~20% clinopyroxene which is probably a sampling issue caused by its relatively large grain size. These 6 samples all have granite-like compositions, i.e., high SiO_2, low FeO, and high alkalis and Ba (Table 1, Figs. 1,2,3).

Table 1. Bulk compositions of 12032,366-19 and selected lunar granites. Oxide units are wt%. Element units are ppm.

	1	2	3	4	5	6
SiO_2	70.0	73.0	70.8	74.2	68.1	75.5
TiO_2	1.04	0.60	0.60	0.33	0.90	0.26
Al_2O_3	13.5	11.9	12.7	12.5	10.2	12.3
FeO	4.93	0.90	6.30	2.32	6.99	3.10
MnO	0.13	0.12	0.10	0.02	-	0.04
MgO	0.14	0.70	0.40	0.07	1.53	0.20
CaO	3.0	1.40	1.00	1.25	4.89	0.50
BaO	0.77	0.65	-	0.24	-	0.61
Na_2O	2.49	1.40	1.10	0.52	0.79	0.53
K_2O	4.5	6.80	7.40	8.60	3.39	7.55
P_2O_5	0.039	-	0.70	-	-	-
ZrO_2	0.203	0.15	-	0.09	-	-
Hf	41.9	24	-	13.9	-	16
Cr	56	1010	0	17	-	70
Nb	287	-	-	-	-	-
Ce	111	126	-	117	-	50
Nd	82	64	-	58	-	34
Y	494	-	-	-	-	-
Th	132	41	-	65	-	9.5
U	45	12.3	-	23.4	-	-
SUM	100.8	97.6	101.1	100.1	96.7	100.6

1. 12032,366-19: This study – microprobe and modal recombination. **2.** 12013,10 light: [6,7,8,9]. **3.** 12070,102-5: Potash rhyolite [10]. **4.** 14321,1027: Pristine granite clast [11]. **5.** 15405,12: Granite fragments [12]. **6.** 73255,27/,3: Felsite clast [13].

Other lunar granites have compositions consistent with mixtures of granite and either KREEP impact melt breccias that host them or quartz monzogabbro.

The most striking difference between 12032,366-19 and the five other granites is that its Na_2O/K_2O is higher by a factor of 2-5 than that of the others – a characteristic reflected by the abundance and sodic nature of its plagioclase [1].

Origins of Lunar Granite: The alkali-rich feldspars and Fe-rich mafics indicate that 12032,366-19 is an extreme product of melt fractionation; however, it is uncertain whether fractional crystallization alone can explain the sample's bulk composition. To explore this, we selected KREEP basalt (KB) 15434,18,199-A (composition compiled by [14]) and basaltic andesite glass (BAG) of Zeigler et al. [15] as compositions to represent potential parent melts. BAG has higher Fe/Mg and higher Al_2O_3. The compositions were modeled as extended fractional crystallization (using MAGFOX [5]) until crystallization reached 98 mol% (KB) and 95 mol% (BAG).

In the KB melt, [SiO_2] increases from ~53 to 55 wt% at 47 mol% crystallization when quartz begins to crystallize. [SiO_2] further increases to ~61 wt% at 98 mol% crystallized. [K_2O] increases to 6.6 wt% at 93 mol% crystallization when K-feldspar (Ab_{15},Or_{81}) begins to

form, and then decreases to 6 wt%. Initially, [Al_2O_3] decreases from ~16 to 12 wt% at 74 mol% crystallization and then increases to 16 wt%. [FeO] remains relatively constant around 10 wt% until quartz forms at ~47 mol% crystallization, after which it rises to 14.5 wt% at 86 mol% crystallization. From there, [FeO] decreases owing to crystallization of fayalitic olivine and ferropyroxene (Fo_{10}, $En_{20}Wo_{10}$).

In the BAG melt, [SiO_2] initially decreases slightly to 52 wt% at 50 mol% crystallization and then increases to ~62.1 wt%. [K_2O] increases from 0.7 wt% to around 6% at 91.5 mol% crystallization. Plagioclase ($An_{86}Ab_{13}$) forms early and initially suppresses Al_2O_3, but Al_2O_3 eventually increases to ~17 wt%. [FeO] remains relatively constant at ~13.5 wt% until silica forms at ~22 mol% crystallization. It then rises to 16 wt% at 50 mol% crystallization. With further crystallization, olivine and pyroxene compositions become increasingly Fe-rich (to Fo_3, En_4Wo_2), leading to a final [FeO] of ~8 wt%.

Even after extended fractional crystallization, residual melts do not reach SiO_2 concentrations of the pristine granite samples. Some other process is needed, such as gravity separation of low and high-density phases. If we take the mineral compositions that are in equilibrium with the KB and BAG residual melts at the last stage of crystallization as modeled above and adjust the proportions by increasing the low-density phases relative to the high-density phases (ignoring phosphates and Zr-Ti oxides), as might occur during density separation, we can get to the compositions of the pristine granites without appealing to SLI. An exception for 12032,366-19 is its high Na_2O, which requires a more sodic plagioclase and a higher Na_2O content in the starting melt composition.

Conclusions: The six granites discussed here differ significantly in composition from one another (e.g. [Na_2O] and [BaO]). These differences may simply result from differing physical accumulations of low-density fractions and trapped melt separated from otherwise similar parent melts. The origin of 12032,366-19 could be explained by extended fractional crystallization of a parent melt of KB or BAG composition with 0.3-0.5 wt.% more Na_2O, which experienced late-stage gravity separation concentrating the lighter silica, plagioclase, and K-feldspar (Figs 1,2,3). Silicate liquid immiscibility [16-19] may not be required; however, preliminary results indicate that the BAG liquid passes into the miscibility gap in the early stages of fractional crystallization.

Acknowledgements: We thank Alian Wang for Raman spectroscopic measurements. This work was funded by NASA grant NNG04GG10G (RLK).

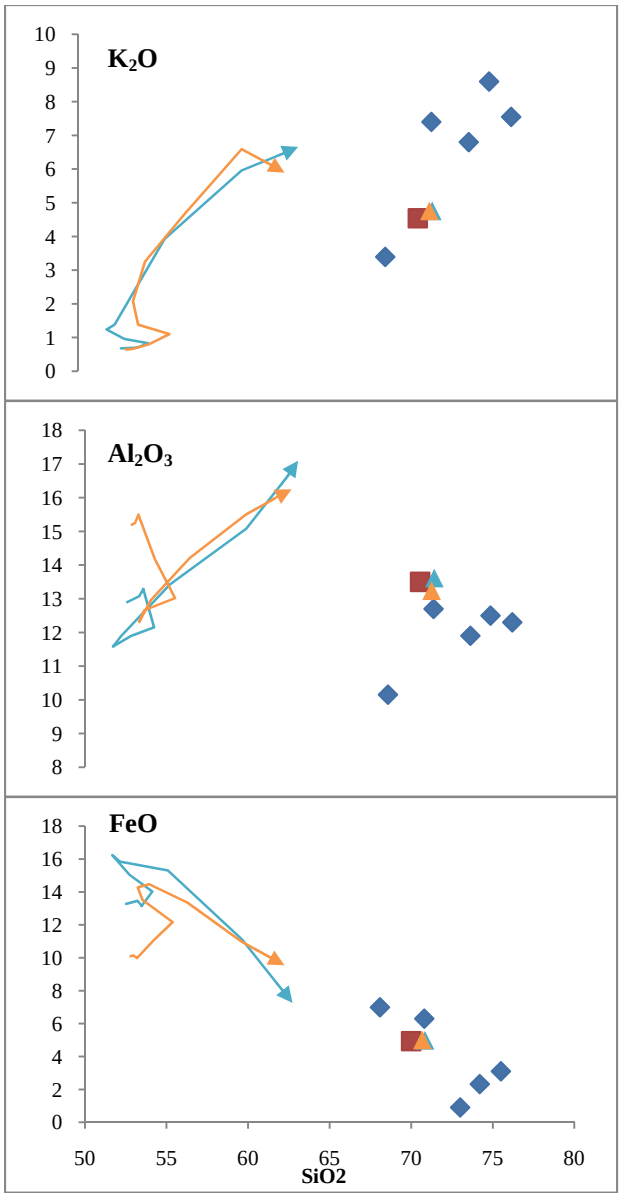

Figures 1, 2, and 3. Red squares represent 12032,366-19. Blue diamonds are the other lunar granites in Table 1. The orange line follows the modeled KB liquid from 0-98 mol% fractional crystalization. The blue line follows the modeled BAG liquid from 0-95 mol% fractional crystalization. Orange and blue triangles represent the solids modelled to be in equilibrium with the melts after these high degrees of crystallization of the KB and BAG melts, respectively, plus gravity separation to enrich the assemblage in low-density phases. Units are wt%.

References: [1] Seddio et al. (2009) *LPS XL*, #2285. [2] Seddio et al. (2009) *LPS XL*, #2415. [3] Korotev R. L. et al. (2002) *LPS XXXIII*, #1395. [4] Korotev, R. L. et al. (2000) *LPS XXXI*, #1363. [5] Longhi (1991) *AM, 76*, 785-800. [6]Quick et al. (1977) *PLPSC18*, 2153-2189. [7] Hubbard et al. (1970) *EPSL, 9*, 181-184. [8] Schnetzler et al. (1970) *EPSL, 9*, 185-192. [9] Wakita and Schmitt (1970) *EPSL, 9*, 169-176. [10] Marvin et al. (1971) *PLPSC2*, 679-699. [11] Warren, P. H. et al. (1983) *EPSL, 64*, 175-185. [12] Ryder (1996) *EPSL, 29*, 255-268. [13] Blanchard and Budahn (1979) *PLPS10*, 803-816. [14] Papike et al. (1998) *Planetary Materials, RIM, 36*, 5-1. [15] Zeigler et al. (2006) *GCA, 70*, 6050-6067. [16] Jolliff (1991) *LPS XXI*, 101-118. [17] Hess et al. (1989) *LPS XX*, 408-409. [18] Rutherford et al. (1976) *PLPSC7*, 1723-1740. [19] Roedder and Weiblen (1970) *PLSC1*, 801-837.